



Automated Transfer Station with Machine Learning Techniques for Twisted Heterostructure Study

Zihang Wang

Advisor: Professor Alex Zettl

Spring 2020

Abstract

A recent discovery of superconductivity in twisted bilayer graphene inspires researchers to study twisted van der Waal (vdW) heterostructures and investigate the mechanism behind the unconventional superconductivity. However, this angle-dependent effect requires accurate control of stacking between vdW layers and minimum sample-to-sample variations, which makes the fabrication process difficult. Therefore, it is crucial to create a standardized technique to produce high-quality twisted stackings of vdW heterostructures with the least effort and time. By having two home-designed automated transfer stations, we have boosted our ability to create different heterostructures and test variety of materials efficiently. By using the technique of unsupervised machine learning (K-mean clustering), we extract and separate the layer dependence of different materials, which reduces the time and effort for identifying desired configuration. On the first part of the thesis, I present two motorized transfer stages assemblies (one digital and one analog). Via Labview interface, multiple visa-communication channels are used to control the transfer stage remotely. A statistical learning (k mean clustering) technique is used to extract different layers of graphene flakes, which increase the efficiency of identification process. On the second half of the thesis, I show the device fabrication technique and some preliminary results of a two-dimensional (2D) material - MoTe₂ that we will investigate in the future.

Background and Motivation

There has been an explosion in research around graphene since its discovery in 2004[1]. Recently, a MIT team (lead by Professor Jarillo-Herrero), successfully turned graphene to a superconductor at 1.7 K by twisting the orientation of the two graphene layers to a certain angle (about 1.1° degree)¹. This fascinating discovery not only provides a new understanding in electron-electron correlations in twisted systems, but also suggests the true mechanism behind the unconventional superconductivity². It also inspires scientists to engage with some novel experimental techniques that triggered other discoveries in twisted vdW systems. However, it is difficult to resolve angle-dependent effects independent of sample-to-sample variations in fabricating a large number of devices³. Thus, new fabrication techniques that enable the accurate and efficient stacking of vdW hetero-structures are desired.

Twisted vdW heterostructures

General Interests in stacked 2D materials

The electronic bandgap is the result of periodic lattice spacing. Semiconductors and insulators' transport and optical properties are highly determined by their bandgap. 2D stacking allows us to create new interface (bandgap) that don't exist in original samples. Since every material (pure or composed) has its unique lattice and potential periodicity, there are almost infinite number of combination that scientists can conduct research on.

Twisted Bilayer graphene

Graphene has a linear energy dispersion with high Fermi velocity (10^6 m/s). When two graphene sheets stack together, it results in a particular stacking order (AA or AB). By twisting the relative angle between top and bottom graphene, a modulated superlattice formed (AA-AB). Depending on the angle magnitude, the superlattice periodicity can be changed. This superlattice yield a periodic potential which folds the band structure into the first mini Brillouin zone¹. Increasing this potential results in the motion of Dirac point toward the mini zone boundary, and opening a bandgap if the potential exceeds a particular energy threshold at boundary. This change in potential will yield the change in Fermi velocity that will be crucial to study electronic properties, particularly at a magic twisting angle.

The Magic Angle stacking

When a particular angle (1.1 degree) makes the Fermi velocity drops to zero at the charge neutrality point¹. It will yield a high effective mass since:

$$m_{eff} \sim \frac{1}{v_{fermi}} \quad (1)$$

Thus, in this magic angle, the high effective mass is one of the explanation of the super flat energy bands near the charge neutrality point. There flats bands thus exhibit Mott insulating states at half-filling¹.

Superconductivity in Magic Angle stacking

By tuning the gate voltage V_g , the carrier density can be controlled. Superconductivity can be realized at the twisted bilayer graphene with the magic angle¹.

Extending twisted angle method to other 2D materials

Currently, twisted angle method is mostly applied to graphene related experiments. In general, different material will have different modulated superlattice structures by twisting the relative angle between two layers. Thus, the experimental richness may lead to some significant discoveries that contribute to the understanding of the unconventional superconductivity.

Device fabrication process

Dry transfer is the backbone in 2D material device fabrication process. The quality of the device is highly depending on this transfer process. Thus, by having a reliable technique in transfer process, researchers can accurately control the stacking and investigate the angle-dependent effects. The fabrication technique follows a series of complex steps, which is showing in Figure 1.

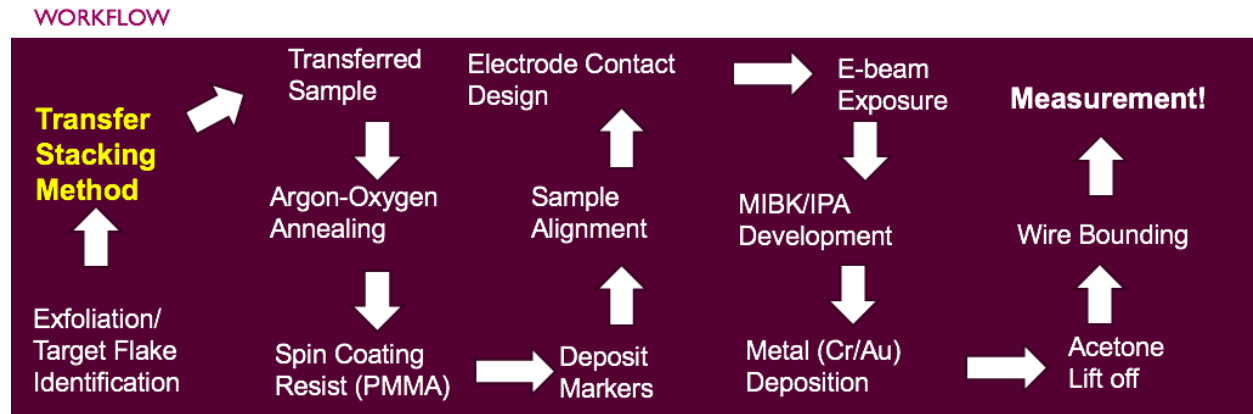


Figure 1: Transfer and device fabrication process

Building Automated Transfer Station

System requirements of automated transfer station

We will modify a probe station by adding three axes motor control as well as thin flake identification and capture functions. Motor control can be accomplished by using Labview program (or other suitable software). The goal is to control the station accurately and remotely. As for the computer and software requirements, Win10 and Labview 2019 are used for controlling the transfer station while Python 3.6 is used in image analysis.

Overview of the transfer station

We used 3 major axes (X-Y-Z directions) that operates independently with the additional angle control. We utilized the four stepper motors that works under the microscope. Since the stepper motors were originally two phase unipolar motors, they did not fit with our design. Thus, we reconfigured the motors into two phase bipolar motors in order to fit the existing diver. The labview program made the automated operations available. By adjusting the stepping size, we found around 25000 step/rotation interval yield the smoothest rotations. The Z-axis moving speed (and temperature) is the most important factor that affects the transfer process and thus the quality of samples. Motorized control during the transfer process will give us the ability to establish a systematic optimized procedure (speed vs quality of samples) for yielding the best quality samples. The following figure (Figure 2) shows the home-configured automated transfer station and graphic flow chart of the transfer station operation.

Labview program and home-designed user interface

Labview program controls the motors via two 2-terminal signal generators. A communication signal sent by the Labview via VISA-communication channel to the signal generators and output accordingly.

1. Signal generator controller subVI program

Figure 3 shows the block diagram of the signal generator communication VI, Which provides a direct communication between the computer and the signal generator. The square wave is used for motor control. The general condition of the signal output consists of 3 components:

- Signal Voltage range:0V-5V

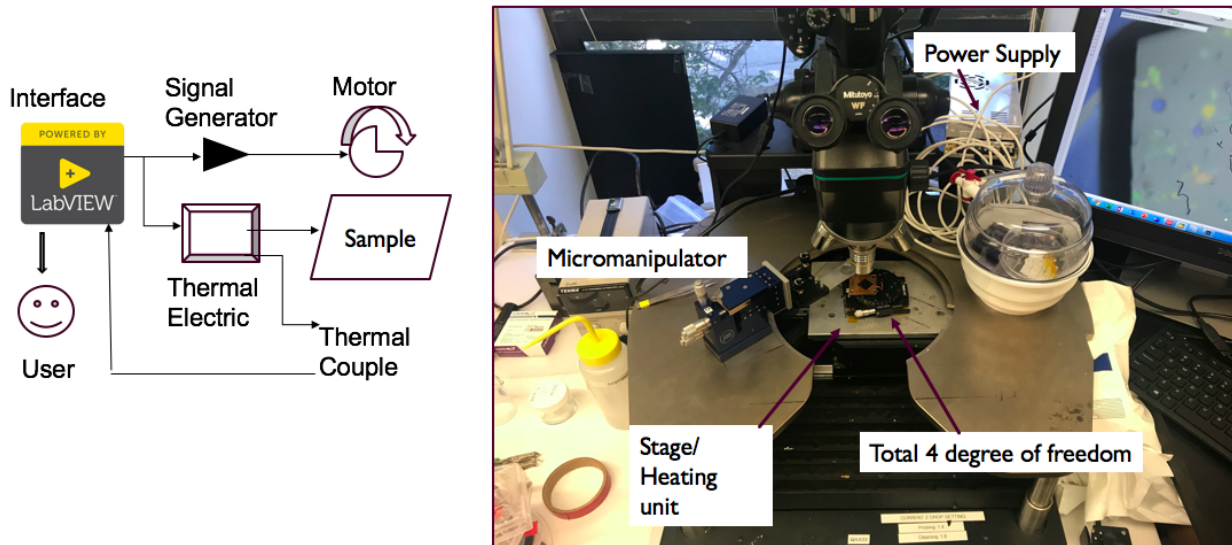


Figure 2: Motorized transfer station and graphic flow chart of the transfer station operation

- Duty Cycle: 80%
- Frequency Range: 2kHz-100kHz

The communication channel block diagram is showing below in Figure 3:

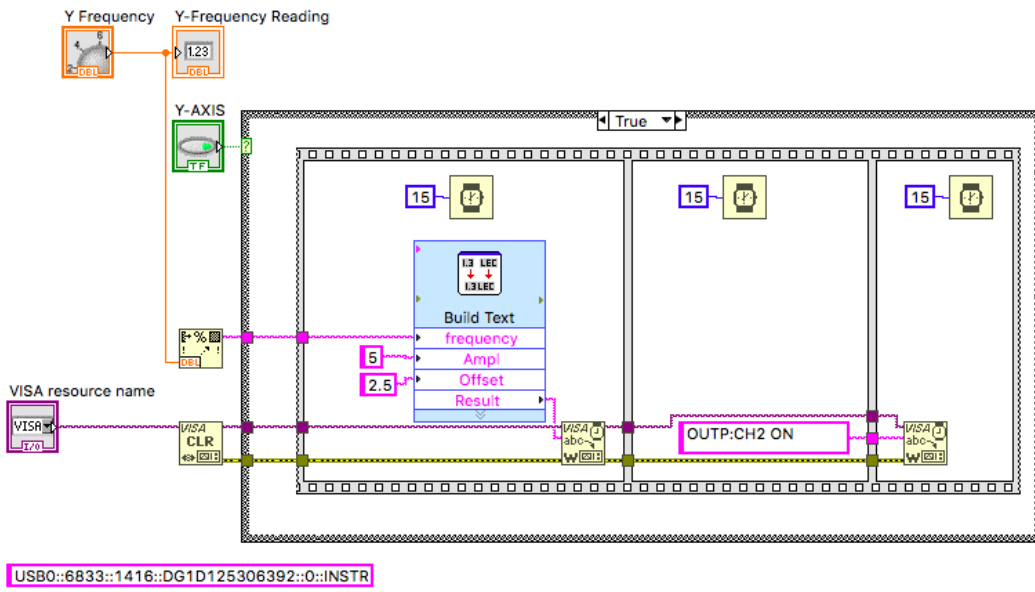


Figure 3: Block Diagram of the communication channel. Inputs include frequency and on-off signal. A sequence was used to ensure the execution follows the exact communication order. The wait may be different on different PC since the waiting time may vary with the communication speed.

2. 4-channel Nesting subVI for motor control

4 sub-VIs were nested in the while loop for motor control. Event structures was used to detect the changes when pressing the control buttons on the user interface. By combining NI digital output with event structure, we make it possible that the VI controls 4-motors independently.

3. Photographic Scanning subVI for automated image capturing

A scanning sub-VI was developed to further help researchers to search for target flakes. The Nikon camera was directly controlled by the Labview program, and photo capture was synchronized with fixed scanning steps. Programming with the camera adds extra flexibility to the standard transfer process.

4. Temperature control PID subVI

A PID controller sub-VI is used to adjust the current in the thermal electric. A temperature feedback loop (thermal couple) was used in this configuration.

Transfer Station Configuration

A 24V DC power supply is used to power the motors. Stepper motors are controlled by DM542E drivers, which allows bipolar connection (A \bar{A} , B \bar{B}). There are 4 inputs on the DM542E driver: pull (\pm) and direction (\pm). The pull (\pm) control the stepping frequency. The input frequency will be sampled and amplified to control the stepper motor. direction (\pm) uses H-bridge microchips which flip the direction upon the polarization of the input signal. In our connection, we first connected pull (\pm) to signal generator output, (a square wave, 5V). Then, NI digital outputs were connected in series with direction (\pm). A programmable power supply was controlled by the PID VI program.

Machinery

Since the original probe station controller uses union-polar stepper configuration, we have to adjust the wiring and inner connections. The micro-manipulator, rotation base, and heating stage are machined as desired with precision of 0.1mm.

(Second transfer stage, an Analog Transfer Stage Development

A new analog transfer station was built with higher precision rotation and position. The focal length was carefully measured to ensure the optimal distance between camera, eyepiece, and samples, which is showing in Figure 4. Comparing to the previous transfer stage, the stability and angle accuracy were improved significantly. NEMA 17 Stepper Motor was used with 12V input voltage. Ceramic heater unit (500C) was used to provide heat to the sample.

Analog control box

The control box used 12V power supply with 3-H bridge logic gates. Positive and negative bias were controlled by analog resistors. Polarity will be switched if an opposite button was pushed. The rotation stage has the gear ratio of 1:120, which has 0.5 degree accuracy. The stage is designed and assembled to ensure the performance. The optical Amscope T490B was used with ThorCam L1000.

Machine Learning Technique for Flake Identification

In order to identify the layer dependence of graphene flakes, we wrote a simple program to detect layer dependency. The program used K-mean Clustering method to group different layer of materials. First, a group of RGB value is collected from the image as 3D numpy array. Then, a 3D clustering sequence (geometric distance convergence) is used to group different clusters. A new label is created for each group. Then, reconstruct the image based on their original position. The following figure shows the basic idea of k-mean clustering, Figure 5 [7]. First, an arbitrary data array was selected as the initial point. Then, the geometric distance was calculated from each center to the RGB datapoints. Then, by assigning the new geometric mean to the initial array, a new distribution is formed. By repeating this procedure, we can converged the center to a stable value (Figure 5, left figure).

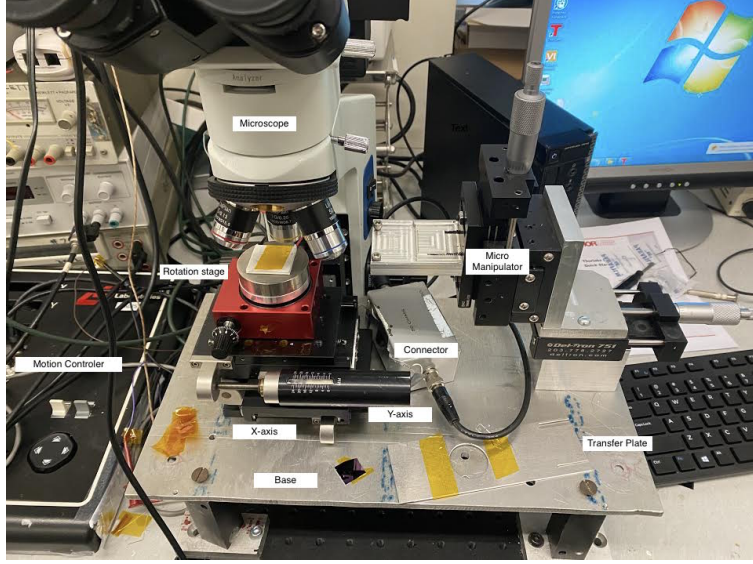


Figure 4: Second home-built analog transfer station

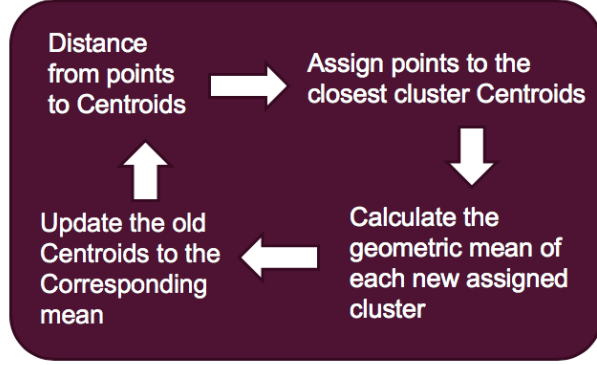


Figure 5: K-mean Clustering Method

Centroid Convergence

We decomposed the picture to its RGB space, and programmed the K-mean values which gives us the following convergence pattern (Used G value for a particular cluster):

Reconstruction

Based on the RGB cluster method, we separate layer dependence, and reconstruct the image based on their layer dependence.

Device Fabrication and Measurements

Next we show the device fabrication and measurements of van der Waal heterostructures based on 2D materials using the above home-built transfer stations. Due to the graphene-like layered structure and high spin-orbit coupling, transition metal dichalcogenides (TMDs) have rich physics in both electric and magnetic properties. The structural richness in TMDs also enables us to study phase transition (Figure 8).



Figure 6: K-mean Clustering Convergence (plot on the left) and RGB (plot on the right) space division. In this typical example, we use 7 cluster centers. Centroid convergence step is around 6.

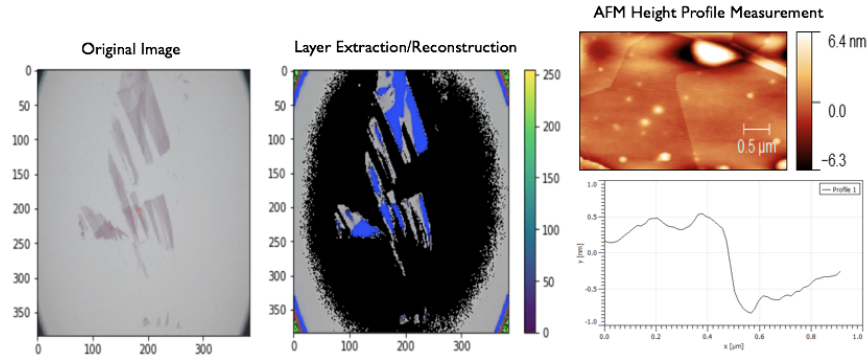


Figure 7: K-mean Clustering Reconstruction. The Original Image has three layers, and the reconstruction identify two. Because of the limited computational power, we reduced the image quality (from 1MB to 100kB). Thus, some of the features did not capture.

TMDs Characteristic Table

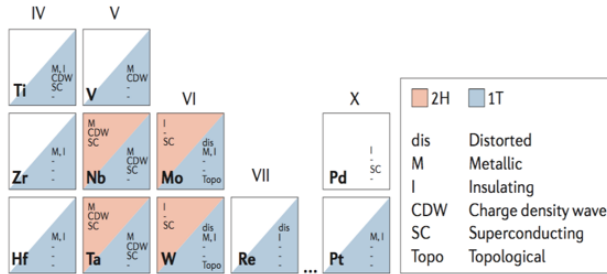


Figure 8: Electric and magnetic properties in TMDs. From Sajedeh Manzeli, *Nature Reviews Materials* volume 2, Article number: 17033 (2017)

Characterization for MoTe₂

We chose MoTe₂ for our study as it has low energy barrier between 2H and 1T' phases.[add refs here] Structure composition and properties of 2H and 1T' phase MoTe₂ are showing below (Figure 12):

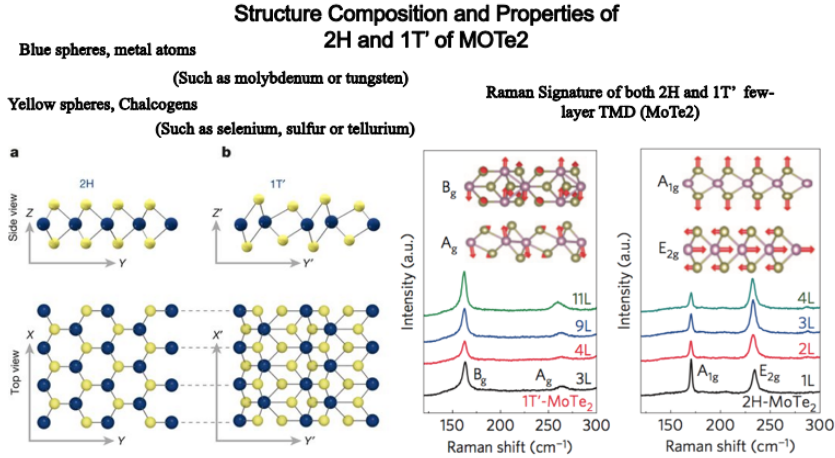


Figure 9: Structure Composition and Properties for both 2H and 1T' MoTe₂. On the left, the Blue spheres represent metal atoms, and the Yellow spheres represent Chalcogens. On the right, it shows the Raman Signature of both 2H and 1T' few-layer TMD (MoTe₂) (Ruppert, (2014)).

Raman identification for MoTe₂ thin layers

Raman technique was used to identify the structure. Our sample shows agreements with 1T' MoTe₂. Note: MoTe₂ 1T' phase is metallic with a distorted 1T crystal structure.

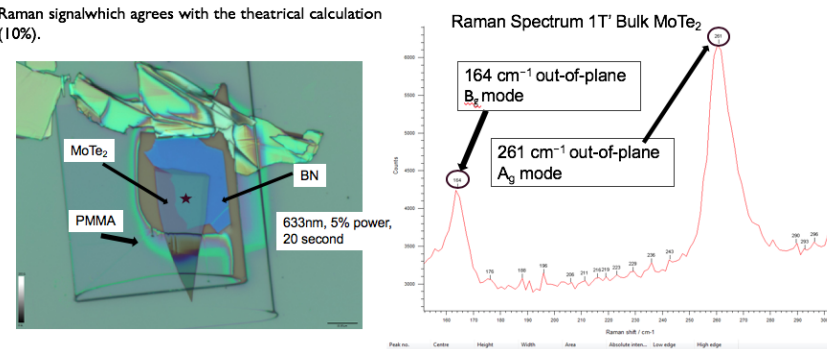


Figure 10: Raman signature of 10-layer MoTe₂. It is consistent with the 1T' phase MoTe₂ that presented in the literature.

Transfer Process and device design for MoTe₂

A particular TMD is interested us: MoTe₂ due to its low phase transition energy barrier. However, MoTe₂ is slightly air sensitive, so the fabrication needs cautions. To avoid oxidation, the flakes are exfoliated in the glovebox with Oxygen less than 1ppm. Then the flakes are identified by optical microscope and labeled accordingly. Sealed container was used to transport the samples. By carefully storing the sample in a vacuum desiccator, we ensure the samples remain stable for a long period of time. With the new transfer stage, several samples with specified twisted angles are transferred and fabricated for measurements. The dry transfer process uses PC polymer and chloroform as PC remover. It can be generalized into 3 steps:

- Exfoliation/Target Flake Identification

-
- Pick-up, Transfer and Stacking
 - Polymer Removing and Argon-Oxygen Annealing

Transferred sample was coated with PMMA950 (spin speed at 2000rpm for 60 seconds). Under the electron microscope, we aligned and patterned via E-beam lithography (EBL) technique.

- Low Dose may lead the pattern incompleteness after the development (underexposure).
- High Dose may lead collapse in the interline after the development (overexposure)

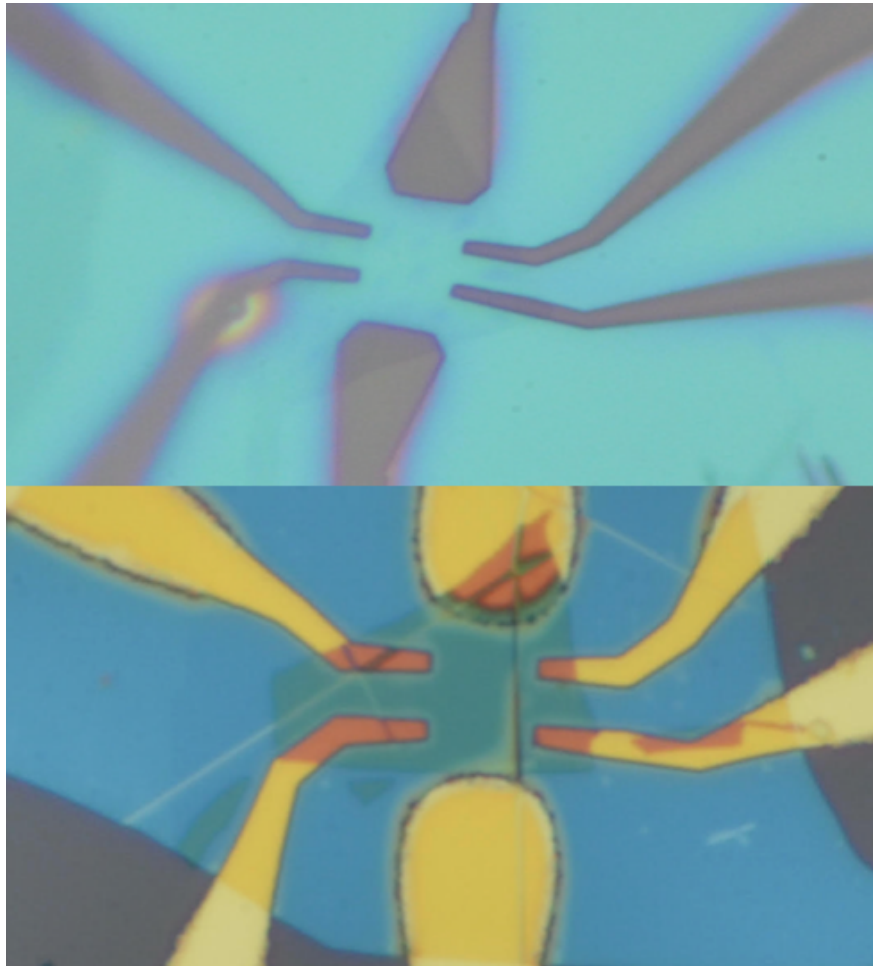


Figure 11: Device structure. The top figure shows the EBL electrodes after the development of MIBK:IPA at a ratio of 1:3. Electrodes are patterned on top of the 3-layer MoTe₂. Bottom figure shows the same electrodes with (10/50nm) Cr/Au evaporation for the metal contacts. Since MoTe₂ is slightly air sensitive, a hBN flake was transferred as a protective layer.

Finally, the device was mounted on the device holder, and prepared for measurements. The contact resistance is relative high (in 150kΩ Range) in this device. In order to perform reliable transport measurements, ohmic contacts are required. Thus, more devices were fabricated with different contact metals to further reduce the contact resistance and investigate angle dependent effects in MoTe₂ vdW heterostructures. The experiments are still in progress and require more time to complete.

Summary and future work for Twisted MoTe₂

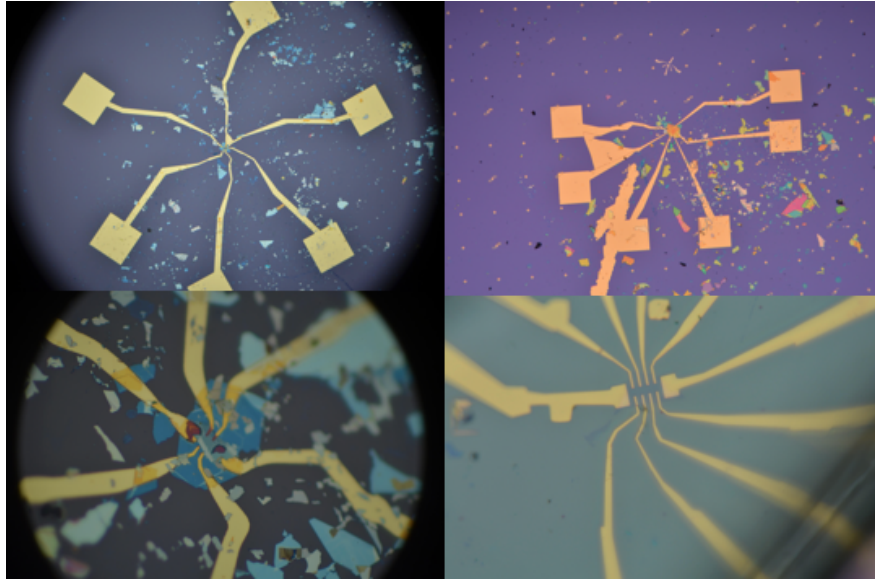


Figure 12: Several MoTe₂ devices are fabricated for measurements.

Two transfer stations were built (angle and position automated control) to further boost our ability to make more reliable twisted vdW heterostructures. A software was developed to extract 2D layers from K-Means Clustering method (Unsupervised machine learning). After careful test of our transfer stations, twisted MoTe₂ samples have been successfully fabricated and prepared for transport measurements. The accuracy of the twisted angle can be precisely controlled and monitored by our home-developed software. In the near future, we will systematically study the angle-dependent effects of twisted MoTe₂ heterostructures by fabricating a large number of devices using our new transfer stations with the machine learning technique. We will also further dope the heterostructures using an e-beam doping technique [add refs here, my Nature electronics paper] and explore possible superconducting properties.

Acknowledgement

I would thank Professor Alex Zettl, Professor Feng Wang, Dr. Wu Shi, Salman Khan, and others who support me on this project.

References

- [1] Cao, Yuan and Fatemi, Valla and Fang, Shiang and Watanabe, Kenji and Taniguchi, Takashi and Kaxiras, Efthimios and Jarillo-Herrero, Pablo. Unconventional superconductivity in magic-angle graphene superlattices. *Nature*. 43–50(2018).
- [2] Gibney E. Surprise graphene discovery could unlock secrets of superconductivity. *Nature*. 151–152 (2018)
- [3] Hamish Johnston. Discovery of ‘magic-angle graphene’ that behaves like a high-temperature superconductor is Physics World 2018 Breakthrough of the Year. *Physics World*. (2018)
- [4] Belle Dumé. ‘Twistronics’ tunes 2D material. *Physics World*. (2018)
- [5] S. Dürr, T. Volz, N. Syassen, D. M. Bauer, E. Hansis, G. Rempe. A Mott-like State of Molecules. 1 (2006).
- [6] Wang, Q. H., Kalantar-Zadeh, K., Kis, A., Coleman, J. N. Strano, M. S. Electronics and optoelectronics of two-dimensional transition metal dichalcogenides. *Nature Nanotech*. 7, 699–712 (2012).

-
- [7] Mark A. McCord, Introduction to Electron-Beam Lithography, Short Course Notes Microlithography 1999, SPIE's International Symposium on Microlithography 14-19 March, 1999; p. 22)
 - [8] Bradley, P. S., Bennett, K. P., Demiriz, A. (2000). Constrained k-means clustering (Technical Report MSR-TR-2000-65). Microsoft Research, Redmond, WA.